

Subspace Multiuser Detection for Multicarrier DS-CDMA

June Namgoong, Tan F. Wong, *Member, IEEE*, and James S. Lehnert, *Fellow, IEEE*

Abstract—A subspace-based linear minimum mean-squared error (MMSE) multiuser detection scheme is proposed for a multicarrier direct-sequence code-division multiple-access (MC-DS-CDMA) system. Typically, a MC-DS-CDMA system employs a band-limited chip waveform. The band-limited nature of the chip waveform causes problem in applying standard subspace techniques because no nonnull noise subspace can be formed. It is shown that channel and timing information needed for the construction of the linear MMSE detector can be identified by a multiple-signal-classification-like algorithm based on a finite-length truncation approximation of the chip waveform. In practice, since perturbed versions of the subspaces assumed in the finite-length truncation approximation are actually observed, and because of the band-limited property of the chip waveform, the accuracy of the channel estimation and, hence, the performance of the MMSE detector are degraded. This effect is investigated in this paper.

Index Terms—Code-division multiple access, multicarrier system, multiuser detection, subspace-based estimation.

I. INTRODUCTION

RECENTLY, there has been considerable interest in multicarrier direct-sequence code-division multiple-access (MC-DS-CDMA) systems, which are known to be effective in frequency-selective fading channels. The MC-DS-CDMA transmission scheme considered in this paper is proposed in [1], where a band-limited direct-sequence (DS) waveform modulates multiple carriers. Kondo and Milstein [1] employ maximal ratio combining (MRC) to combine the desired signal contributions from different carriers. Lok *et al.* [2] show that when the noises and interference are correlated, MRC is not optimal. They propose an adaptive algorithm to take advantage of this correlation to reject multiple-access interference (MAI). Their method can be viewed as a form of minimum mean-squared error (MMSE) multiuser detection in the frequency domain. Since the number of carriers is usually not large, this form of frequency-domain multiuser detection performs best in situations where only a few strong interferers

are present. Since the MC-DS-CDMA system also contains direct-sequence components, traditional (time-domain) multiuser detection [3]–[5] can be performed on each of the carriers to improve the effectiveness of the frequency-domain scheme for cases where there are a large numbers of strong interferers.¹ A more direct, and probably better, approach is to perform joint time and frequency domain multiuser detection.²

The major difficulty encountered in such a time-frequency multiuser detection scheme is that a large amount of channel information, such as the timing and fading coefficients of the users, is needed. A promising and recently proposed approach for obtaining these channel estimates is to use subspace-based estimation techniques [6]–[12].

We propose a subspace-based MMSE receiver for a MC-DS-CDMA system. The orthogonality between the *noise subspace* and the desired signal vector is exploited to blindly extract the timing and channel required for the construction of the linear MMSE detector. This idea is similar to those in [10] and [11], which consider the channel estimation and multiuser detection for a single-carrier DS-CDMA system.

While the use of subspace techniques for MC-DS-CDMA systems is an extension from single-carrier systems, the band-limited property of MC-DS-CDMA signals significantly affects the effectiveness of the subspace technique. This fact has not been addressed in all the work on single-carrier CDMA systems mentioned above. The operation of any subspace-based technique requires a nonnull noise subspace. For a time-limited chip waveform, which is usually assumed in single-carrier CDMA systems [6]–[12], the number of *signal vectors* (see Section III) from each user is finite. Hence, by taking a sufficient number of samples of the received signal, a nonnull noise subspace can be obtained. However, MC-DS-CDMA systems employ band-limited chip waveforms, which contribute an infinite number of signal vectors that span the entire space, regardless of the number of samples taken. Hence, a nonnull noise subspace cannot be formed. To circumvent this difficulty, we limit the number of signal vectors by neglecting the tail of the chip waveform. Based on this approximation, we form the (nonnull) signal and noise subspaces needed for the proposed subspace-based multiuser detection technique. The effect of this approximation is investigated by matrix perturbation analysis techniques. In particular, we investigate the effects of the vectors which are ignored by the finite-length approximation of the chip waveform on the observed subspaces and, hence, the proposed subspace-based estimation method. The vectors ignored by finite-length

Paper approved by U. Madhow, the Editor for Spread Spectrum of the IEEE Communications Society. Manuscript received February 17, 1999; revised February 10, 2000. This work was supported by the U.S. Defense Advanced Research Project Agency (DARPA) GloMo Project AO F383, AFRL Contract F30602-97-C-0314. This paper was presented in part at the IEEE Wireless Communications and Networking Conference, New Orleans, LA, September 21–24, 1999.

J. Namgoong and J. S. Lehnert are with the School of Electrical and Computer Engineering, Purdue University, West Lafayette, IN 47907-1285 USA (e-mail: lehnert@purdue.edu).

T. F. Wong is with the Department of Electrical and Computer Engineering, University of Florida, Gainesville, FL 32611-6130 USA (e-mail: twong@ece.ufl.edu).

Publisher Item Identifier S 0090-6778(00)09874-3.

¹Since [2] assumes the use of long random signature sequences, this property of the MC-DS-CDMA system is not exploited.

²Short sequences are required in this case.

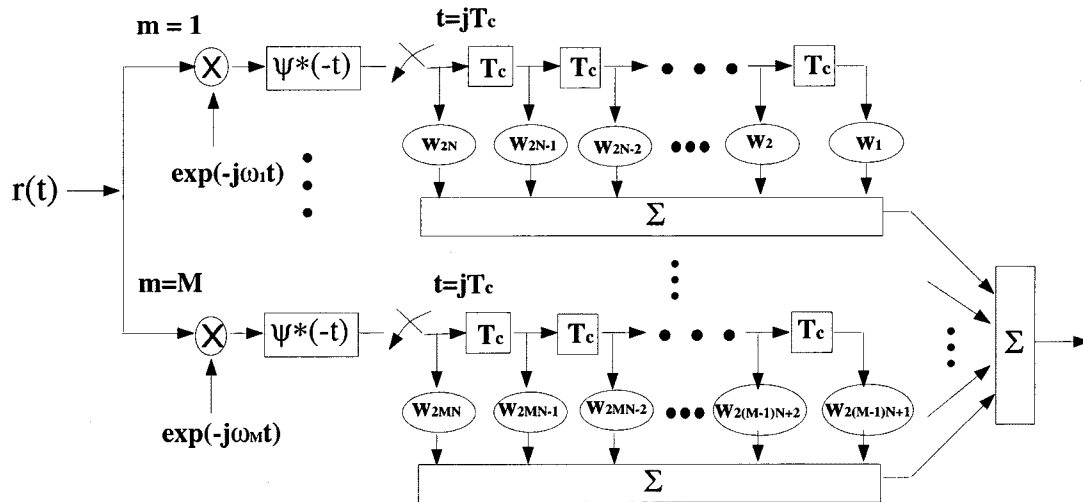


Fig. 1. MMSE receiver in the MC-DS-CDMA system.

approximation cause performance degradation of the subspace-based estimator. Furthermore, we note that, since the chip waveform is not time-limited, the near-far resistance of the linear MMSE detector is *zero* [5]. However, numerical results show that the proposed channel estimation and detection scheme is robust to moderate near-far problems. Moreover, the perturbation analysis indicates that by employing a fast decaying chip waveform and properly selecting a signal subspace dimension, we can obtain reasonably good performance in mild near-far situations.

The rest of the paper is organized as follows. The system model for the proposed MC-DS-CDMA system is introduced in Section II. A linear MMSE detector is developed in Section III. In Section IV, a subspace-based blind algorithm is developed to estimate the fading coefficients needed for the linear detector obtained in Section III. Timing estimation for the desired user is also discussed. We present numerical results to illustrate the performance of the timing and channel estimation and detection schemes in Section V. In Section VI, the effect of the finite-length chip waveform truncation on the noise subspace estimation and, hence, the performance of the proposed algorithm is investigated. Conclusions are drawn in Section VII.

II. SYSTEM MODEL

In this section, we describe the model of the MC-DS-CDMA system. We assume that there are K simultaneous users in the system, and each user uses the same M carriers. The k th user, for $1 \leq k \leq K$, generates a stream of data symbols $b^{(k)} = (\dots, b_0^{(k)}, b_1^{(k)}, b_2^{(k)}, \dots)$. The data symbols $b_j^{(k)}$ are independent random variables with $E[b_j^{(k)}] = 0$ and $E[|b_j^{(k)}|^2] = 1$.

The transmitted signal of the k th user is given by

$$\text{Re} \left[\sum_{m=1}^M \sqrt{2P_k} \left\{ \sum_{i=-\infty}^{\infty} b_i^{(k)} a_{k,m}(t - iT) \right\} e^{j\omega_m t} \right]$$

where

$$a_{k,m}(t) = \sum_{l=0}^{N-1} a_l^{(k,m)} \psi(t - lT_c) \quad (1)$$

is the spreading waveform for the m th carrier of the k th user. The parameter T_c is the separation between consecutive chips. There are N chips per symbol as indicated in (1), and the symbol duration T is related to T_c by $T = NT_c$. Each band is assumed to experience slowly varying flat fading [1]. The parameter P_k is the power for each carrier of the k th user signal, and ω_m is the frequency of the m th carrier. We assume that the chip waveform $\psi(t)$ is band-limited, and the carrier frequencies are well separated so that adjacent frequency bands do not interfere with each other. We also assume $\psi(t)$ is normalized so that $\int_{-\infty}^{\infty} |\psi(t)|^2 dt = T_c$.

The received signal in complex analytic form is given by

$$r(t) = \sum_{k=1}^K \sum_{m=1}^M \sqrt{2P_k} \alpha_{k,m} \times \left\{ \sum_{i=-\infty}^{\infty} b_i^{(k)} a_{k,m}(t - iT - T_k) \right\} e^{j\omega_m t} + n(t) \quad (2)$$

where $\alpha_{k,m}$ accounts for the overall effects of phase shifts and fading for the m th carrier of the k th user, $T_k \in [0, T)$ represents the delay of the k th user signal with respect to the start of the observation interval, and $n(t)$ represents additive white Gaussian noise (AWGN). We assume that the channel coefficients $\alpha_{k,m}$ and T_k vary slowly. Without loss of generality, we consider the signal from the first user as the desired signal and the signals from all other users as interfering signals throughout the paper.

The receiver is shown in Fig. 1. There are M branches in the receiver. Each branch consists of a demodulator and a chip-matched filter, and is responsible for demodulating one carrier. The output of the chip-matched filter on each branch is sampled every T_c s. We observe the chip-matched filter outputs for a duration of $2T$ s so that one complete symbol of the desired user is guaranteed to be observed.

Without loss of generality, let us focus on the detection of the zeroth symbol of the first user, $b_0^{(1)}$. At the m th branch, the output of the matched filter at time jT_c is given by

$$r_m[j] = \int_{-\infty}^{\infty} r(t) \psi^*(t - jT_c) e^{-j\omega_m t} dt. \quad (3)$$

The output sample $r_m[j]$ on the m th branch can be decomposed into different components

$$r_m[j] = \sum_{k=1}^K i_{k,m}[j] + n_m[j] \quad (4)$$

where $n_m[j]$ denotes the component due to AWGN, and

$$i_{k,m}[j] = \sqrt{2P_k} \alpha_{k,m} \sum_{i=-\infty}^{\infty} \sum_{l=0}^{N-1} b_i^{(k)} a_l^{(k,m)} \times \hat{\psi}((j-l-iN)T_c - T_k) \quad (5)$$

is the component due to the k th user signal, for $k = 1, 2, \dots, K$. In (5), the function $\hat{\psi}(\cdot)$ is the output of the chip waveform through the chip-matched filter, i.e., $\hat{\psi}(t) = \int_{-\infty}^{\infty} \psi(s)\psi^*(s-t)ds$. To avoid interchip interference for the desired signal when it is chip-synchronous, the chip waveform is chosen to satisfy the Nyquist criterion, i.e., $\hat{\psi}(nT_c) = T_c$ for $n = 0$ and $\hat{\psi}(nT_c) = 0$ for $n \neq 0$. We vectorize the observations by defining $2N$ -dimensional vectors

$$\mathbf{r}_m = [r_m[0], r_m[1], \dots, r_m[2N-1]]^T \quad (6)$$

$$\mathbf{n}_m = [n_m[0], n_m[1], \dots, n_m[2N-1]]^T \quad \text{and} \quad (7)$$

$$\mathbf{i}_{k,m} = [i_{k,m}[0], i_{k,m}[1], \dots, i_{k,m}[2N-1]]^T \quad (8)$$

for $m = 1, 2, \dots, M$ and $k = 1, 2, \dots, K$. Then, we concatenate the vectors from the M carriers to form the following $2MN$ -dimensional observation vectors: $\mathbf{r} = [\mathbf{r}_1^T, \mathbf{r}_2^T, \dots, \mathbf{r}_M^T]^T$, $\mathbf{n} = [\mathbf{n}_1^T, \mathbf{n}_2^T, \dots, \mathbf{n}_M^T]^T$, and $\mathbf{i}_k = [\mathbf{i}_{k,1}^T, \mathbf{i}_{k,2}^T, \dots, \mathbf{i}_{k,M}^T]^T$ for $k = 1, 2, \dots, K$. Now, (4) can be rewritten as

$$\mathbf{r} = \sum_{k=1}^K \mathbf{i}_k + \mathbf{n} \quad (9)$$

where \mathbf{n} is a zero-mean Gaussian random vector with covariance $\sigma^2 \mathbf{I}_{2MN}$.

The observation vector \mathbf{r} is used to perform timing synchronization and channel estimation. Once synchronization and channel estimation are completed, \mathbf{r} is weighted by a weight vector $\mathbf{w} = [w_1, w_2, \dots, w_{2MN}]^T$ to give a decision statistic based on the MMSE principle, which will be described in Section III.

III. SUBSPACE MMSE DETECTOR

First, let us represent the received vector \mathbf{r} in a more convenient way. We define, for $k = 1, \dots, K$, the $2MN \times 2MN$ diagonal matrix

$$\mathbf{D}_k = \text{diag} \left(\underbrace{d_{k,1}, \dots, d_{k,1}}_{2N}, \dots, \underbrace{d_{k,M}, \dots, d_{k,M}}_{2N} \right) \quad (10)$$

where, for $m = 1, 2, \dots, M$, $d_{k,m} \triangleq \sqrt{2P_k} \alpha_{k,m}$ incorporates the power, phase shifts, and fading for the m th carrier of the

k th user. Moreover, we define, for $k = 1, 2, \dots, K$, and $m = 1, 2, \dots, M$

$$\mathbf{a}_{k,m} = \left[a_0^{(k,m)}, a_1^{(k,m)}, \dots, a_{N-1}^{(k,m)}, \underbrace{0, \dots, 0}_N \right]^T \quad (11)$$

which is a vector of length $2N$ consisting of the N elements of the spreading sequence of the k th user followed by N zeros. Following the notation in [13], we let \mathbf{T}_L and \mathbf{T}_R denote the acyclic left shift operator and the acyclic right shift operator operating on vectors of length $2N$, respectively. We use \mathbf{T}_L^n and \mathbf{T}_R^n to denote n applications of the corresponding operators, resulting in n left and right shifts, respectively. Based on these operators, we define, for $k = 1, 2, \dots, K$, $m = 1, 2, \dots, M$, and every integer i

$$\mathbf{v}_{i,k,m} = \sum_{l=0}^{2N-1} \hat{\psi}((l-iN-\gamma_k)T_c - \tau_k) \mathbf{T}_R^l \mathbf{a}_{k,m} + \sum_{l=1}^{N-1} \hat{\psi}((-l-iN-\gamma_k)T_c - \tau_k) \mathbf{T}_L^l \mathbf{a}_{k,m} \quad (12)$$

where $\gamma_k \in \{0, 1, \dots, N-1\}$ and $\tau_k \in [0, T_c)$ are obtained from the decomposition $T_k = \gamma_k T_c + \tau_k$, for $k = 1, 2, \dots, K$. As before, for each $k = 1, 2, \dots, K$ and integer i , we concatenate the M vectors $\mathbf{v}_{i,k,m}$ to form the $2MN$ -dimensional vector

$$\mathbf{v}_{i,k} = [\mathbf{v}_{i,k,1}^T, \mathbf{v}_{i,k,2}^T, \dots, \mathbf{v}_{i,k,M}^T]^T. \quad (13)$$

With these definitions, we can rewrite (9) as

$$\mathbf{r} = \sum_{k=1}^K \mathbf{D}_k \sum_{i=-\infty}^{\infty} b_i^{(k)} \mathbf{v}_{i,k} + \mathbf{n}. \quad (14)$$

We observe from (14) that \mathbf{r} is a linear combination of an infinite number of vectors in general. This leaves the noise subspace with only the zero vector. To tackle this problem, we note that a fast decaying $\hat{\psi}(t)$ should be chosen in practice. Based on this practical consideration, we assume that the chip waveform decays fast enough so that a given symbol makes a significant contribution only to $2L$ ($L \geq 1$) adjacent symbols. Under this assumption, we neglect the vectors in (14) except for those corresponding to $b_{-L}^{(k)}, \dots, b_0^{(k)}, \dots, b_L^{(k)}$ for the k th user, since these $2L+1$ vectors are the dominant terms³ for \mathbf{i}_k . In other words, each user contributes at most $2L+1$ vectors. Further discussion on this finite-length truncation approximation is given in Section VI.

Now, the received vector is approximated as

$$\mathbf{r} = \sum_{k=1}^K \sum_{l=-L}^L b_l^{(k)} \mathbf{D}_k \mathbf{v}_{l,k} + \mathbf{n}. \quad (15)$$

For notational convenience, we write (15) using a *equivalent synchronous model* described in [4] as

$$\mathbf{r} = \sum_{k=1}^P b_k \mathbf{p}_k + \mathbf{n}. \quad (16)$$

³When $T_k = 0$, only $\mathbf{v}_{0,k}$ and $\mathbf{v}_{1,k}$ are nonzero.

In this model, b_1 corresponds to the desired symbol $b_0^{(1)}$ and $\mathbf{p}_1 = \mathbf{D}_1 \mathbf{v}_{0,1}$. Other vectors correspond to the intersymbol interference and multiple-access interference vectors in (15). We note that $2K \leq P \leq (2L+1)K$.⁴ The following spectral decomposition of the correlation matrix of \mathbf{r} is important for the development of subspace-based channel estimation and detection techniques. The correlation matrix is

$$\mathbf{R} = E[\mathbf{r}\mathbf{r}^H] = \mathbf{S}\mathbf{S}^H + \sigma^2 \mathbf{I}_{2MN} \quad (17)$$

where $\mathbf{S} = [\mathbf{p}_1, \dots, \mathbf{p}_P]$. If we choose different spreading sequences for different users, $\mathbf{p}_1, \dots, \mathbf{p}_P$ are usually (but not guaranteed to be) linearly independent. From now on, we assume that these vectors are, in fact, linearly independent and the chip waveform decays fast enough such that $P < 2MN$. Hence, $\text{rank}(\mathbf{S}) = \text{rank}(\mathbf{S}\mathbf{S}^H) = P$. The spectral decomposition of the correlation matrix \mathbf{R} is given by

$$\mathbf{R} = \mathbf{U}\mathbf{\Lambda}\mathbf{U}^H = [\mathbf{U}_s \quad \mathbf{U}_n] \begin{bmatrix} \mathbf{\Lambda}_s & \\ & \mathbf{\Lambda}_n \end{bmatrix} \begin{bmatrix} \mathbf{U}_s^H \\ \mathbf{U}_n^H \end{bmatrix} \quad (18)$$

where $\mathbf{U} = [\mathbf{U}_s \quad \mathbf{U}_n]$, $\mathbf{\Lambda} = \text{diag}(\mathbf{\Lambda}_s, \mathbf{\Lambda}_n)$, $\mathbf{\Lambda}_s = \text{diag}(\lambda_1, \lambda_2, \dots, \lambda_P)$, and $\mathbf{\Lambda}_n = \sigma^2 \mathbf{I}_{2MN-P}$.

Above, the eigenvalues of \mathbf{R} are arranged in descending order. We define the subspace spanned by the columns of \mathbf{U}_s as the *signal subspace* and the subspace spanned by the columns of \mathbf{U}_n as the *noise subspace*. We note that the signal subspace is just the column space of the matrix \mathbf{S} . Using the results above, it is easy to see that

$$\mathbf{R}^{-1} = \mathbf{U}\mathbf{\Lambda}^{-1}\mathbf{U}^H = \mathbf{U}_s\mathbf{\Lambda}_s^{-1}\mathbf{U}_s^H + \mathbf{U}_n\mathbf{\Lambda}_n^{-1}\mathbf{U}_n^H. \quad (19)$$

Now, we have all the necessary tools to develop a subspace-based linear MMSE detector for the MC-DS-CDMA system. Assuming that the timing of the desired user has been acquired (i.e., the value of T_1 is known), the linear MMSE detector for the zeroth bit of the desired user $b_0^{(1)}$ is obtained by solving the optimization problem below

$$\mathbf{w}^* = \arg \min_{\mathbf{w}} E \left[\left| b_0^{(1)} - \mathbf{w}^H \mathbf{r} \right|^2 \right]. \quad (20)$$

The optimal weight vector \mathbf{w}^* is given by

$$\mathbf{w}^* = \mathbf{R}^{-1} \mathbf{p}_1. \quad (21)$$

Based on (19) and the fact that \mathbf{p}_1 is orthogonal to the noise subspace, we obtain

$$\mathbf{w}^* = \mathbf{U}_s \mathbf{\Lambda}_s^{-1} \mathbf{U}_s^H \mathbf{p}_1 = \mathbf{U}_s \mathbf{\Lambda}_s^{-1} \mathbf{U}_s^H \mathbf{D}_1 \mathbf{v}_{0,1}. \quad (22)$$

In order to implement the MMSE detector described in (22), we need to estimate the signal subspace as well as \mathbf{p}_1 . Given the spreading sequence of the desired user, we need to estimate channel coefficients $d_{1,1}, \dots, d_{1,M}$ and the delay T_1 from the observation vectors and construct $\mathbf{p}_1 = \mathbf{D}_1 \mathbf{v}_{0,1}$ based on

⁴Zero vectors in (15) are not included in (16). The exact value of P depends on how many users are bit- or chip-synchronous ($\tau_k = 0$) to the start of the observation interval. The value of $P = 2K$ represents the best case scenario in which all the users are bit-synchronous to the start of the observation interval. In the worst case scenario, where no user is chip-synchronous to the start of the observation interval, $P = (2L+1)K$.

(12). The performance of the detector depends on the accuracy of these estimations. Methods to perform required channel and timing estimation are given in Section IV.

IV. CHANNEL AND TIMING ESTIMATION

In this section, we describe techniques to estimate the channel coefficients and timing of the desired user, which are both needed in order to implement the linear MMSE detector.

First, we assume that the desired user timing estimation is achieved by a separate process, i.e., T_1 is known. We can estimate the channel coefficients of the desired user by projecting the desired user vector onto the noise subspace [6]–[11]. This approach is similar to the well-known multiple-signal-classification (MUSIC) algorithm in array signal processing applications. Since \mathbf{p}_1 is orthogonal to the noise subspace

$$\mathbf{U}_n^H \mathbf{p}_1 = \mathbf{0}. \quad (23)$$

Equivalently, we can rewrite (23) as

$$\mathbf{U}_n^H \mathbf{V}_1 \mathbf{d}_1 = \mathbf{0} \quad (24)$$

where

$$\mathbf{V}_1 = \begin{bmatrix} \mathbf{v}_{0,1,1} & & & \\ & \mathbf{v}_{0,1,2} & & \\ & & \ddots & \\ & & & \mathbf{v}_{0,1,M} \end{bmatrix} \quad (25)$$

and $\mathbf{d}_1 = [d_{1,1}, d_{1,2}, \dots, d_{1,M}]^T$ is the unknown vector representing the channel coefficients of M carriers of the desired user. Since the column space of \mathbf{V}_1 intersects with the column space of \mathbf{U}_s , which is the null space of \mathbf{U}_n^H , (24) must have a nontrivial solution. If the intersection between the column spaces of \mathbf{U}_s and \mathbf{V}_1 is one-dimensional, then \mathbf{d}_1 can be uniquely determined up to a multiplicative constant. This requires⁵ $P+M \leq 2MN+1$, or $P \leq (2N-1)M+1$, since the column space of \mathbf{V}_1 is M -dimensional. A tighter necessary condition on P can be found by noting the number of equations and unknowns in (24). Since $\mathbf{U}_n^H \mathbf{V}_1$ has $2MN-P$ rows, \mathbf{d}_1 can be uniquely determined up to a multiplicative constant only if $M \leq 2MN-P$, or $P \leq (2N-1)M$. Assuming the worst case scenario that $P = (2L+1)K$, a necessary condition on the number of users for unique determination of \mathbf{d}_1 is then

$$K \leq \frac{(2N-1)M}{2L+1}. \quad (26)$$

We note that the channel estimation technique described above is near-far resistant because the noise subspace does not depend on the powers of the users. However, we also emphasize that this conclusion is based on the approximation that there are only a finite number of vectors contributing to \mathbf{r} . A more detailed discussion on the effect of this approximation on the performance of the channel estimator in near-far scenarios is given in Section VI.

In practice, \mathbf{R} is replaced by its time-average estimate $\hat{\mathbf{R}}$. We perform spectral decomposition on $\hat{\mathbf{R}}$ to obtain an estimate

⁵This follows from the fact that $\dim(\mathcal{S}) + \dim(\mathcal{V}) = \dim(\mathcal{S} + \mathcal{V}) + \dim(\mathcal{S} \cap \mathcal{V})$, where \mathcal{S} and \mathcal{V} denote the column spaces of \mathbf{U}_s and \mathbf{V}_1 , respectively.

of noise subspace $\hat{\mathbf{U}}_n$, which is employed to solve the channel estimation problem above. Due to the presence of thermal noise, the column space of \mathbf{V}_1 may not intersect with the null space of $\hat{\mathbf{U}}_n^H$ and, hence, (24) may not have a nontrivial solution. To avoid this difficulty, we obtain a channel estimate $\hat{\mathbf{d}}_1$ by the following least square approach:

$$\hat{\mathbf{d}}_1 = \arg \min_{\|\mathbf{d}\|=1} \left\| \hat{\mathbf{U}}_n^H \mathbf{V}_1 \mathbf{d} \right\|^2. \quad (27)$$

It is easy to see that $\hat{\mathbf{d}}_1$ in (27) is given by the eigenvector corresponding to the smallest eigenvalue of the matrix $\mathbf{V}_1^H \hat{\mathbf{U}}_n \hat{\mathbf{U}}_n^H \mathbf{V}_1$. We note that in order to demodulate the desired symbol, the amplitude and phase ambiguities (with respect to the real desired user channel vector \mathbf{d}_1) in the estimate $\hat{\mathbf{d}}_1$ must be resolved. One way to avoid this is to employ PSK modulation with differential encoding and decoding.

If the value of T_1 is not available, joint timing and channel estimation for the desired user must be performed. The basic idea is to hypothesize a value for $T_1 \in [0, T]$ and construct the matrix $\mathbf{V}_1(T_1)$ ⁶ based on this hypothesized value. Then, the minimization problem in (27) is solved to get the best estimate $\hat{\mathbf{d}}_1(T_1)$ for this T_1 . The process is repeated for different values of T_1 and the timing estimate \hat{T}_1 is obtained as the solution to the following minimization problem:

$$\hat{T}_1 = \arg \min_{T_1 \in [0, T]} C(T_1) \quad (28)$$

where $C(T_1)$ is the minimization cost function defined by

$$C(T_1) = \frac{\left\| \hat{\mathbf{U}}_n^H \mathbf{V}_1(T_1) \hat{\mathbf{d}}_1(T_1) \right\|^2}{\left\| \mathbf{V}_1(T_1) \hat{\mathbf{d}}_1(T_1) \right\|^2}. \quad (29)$$

The corresponding channel estimate is $\hat{\mathbf{d}}_1(\hat{T}_1)$. Of course, the infinite number of possible hypothesized values of T_1 in the interval $[0, T]$ must be quantized to a finite set in practice. We note that the optimization problem in (28) is one-dimensional. Not all choices of the pair (T_1, \mathbf{d}_1) are allowed. As described above, given a hypothesized value of T_1 , we choose the least square solution $\hat{\mathbf{d}}_1(T_1)$ to (27). Hence, the set of candidate solution pairs are $(T_1, \hat{\mathbf{d}}_1(T_1))$ for all $T_1 \in [0, T]$. The advantage of this formulation is that the search space is greatly reduced, making the method more practical. Moreover, since $C(T_1)$ is a continuous function of T_1 , it must have a minimum on the compact interval $[0, T]$. Hence, if we search fine enough, we are guaranteed to get close to the optimal choice of T_1 that minimizes the cost function.

After acquiring estimates of \mathbf{d}_1 and T_1 , we can either construct the MMSE detector as shown in (22) directly, or adjust the sampling time according to the estimated value of T_1 to resample the chip-matched filter outputs and then repeat the subspace construction by setting $T_1 = 0$. The former approach causes significant loss in signal energy due to chip asynchronism. As suggested in [4] and [13], this can be alleviated by oversampling the chip-matched filter output. The

⁶Here we employ the notation $\mathbf{V}_1(T_1)$ to emphasize the fact that the matrix \mathbf{V}_1 is a function of T_1 .

TABLE I
SIX SAMPLE SYSTEMS

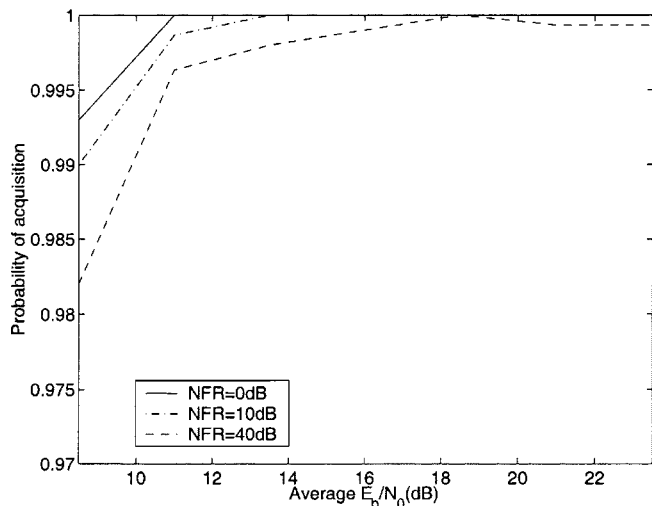
System	K	M	N	near-far ratio (dB)
A	5	4	8	0
B	5	2	16	0
C	5	4	8	10
D	5	2	16	10
E	5	4	8	40
F	5	2	16	40

latter approach gives better performance because not only is the received energy increased, but also the intersymbol interference from the desired user itself is removed. The disadvantage of this method is that the same correlation matrix cannot be used to demodulate the signal of the desired user. When batch eigenvalue decomposition (EVD) of the sample correlation matrix or batch singular value decomposition (SVD) of the data matrix is employed to estimate the signal and noise subspaces, the proposed timing and channel estimation in its current form is computationally expensive. EVD of the correlation matrix requires $O((2MN)^3)$ operations. In addition, the timing estimation algorithm has a computational complexity of $O(M^3)$ per hypothesis based on batch EVD. However, once a noise subspace is estimated, an algorithm of gradient descent type ($O(M^2)$) [12] can be applied to solve the optimization problem in (27) to reduce the computational burden of estimating the minimum eigenvector. Note that the number of hypothesized values of T_1 has no effect on the observed samples. No matter how finely we hypothesize T_1 , we are still using the same estimated noise subspace for all the hypotheses. Of course, we still need to generate all the $\mathbf{v}_{i,k,m}$, which depend on T_1 according to (12), to construct \mathbf{V}_1 . The same amount of storage is required, regardless of the number of hypotheses, if \mathbf{V}_1 is calculated for each hypothesis. Alternatively, we can store all $\mathbf{v}_{i,k,m}$ for all hypotheses for a table lookup. Then, the storage requirement is proportional to the number of hypotheses at the cost of computational efficiency.

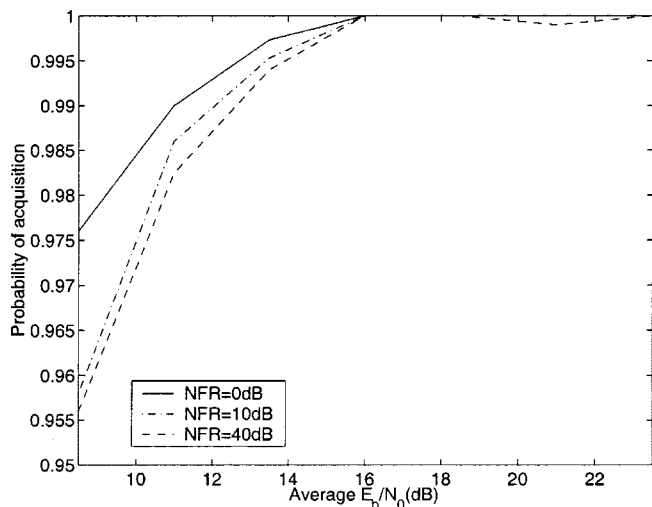
V. NUMERICAL RESULTS

In this section, we investigate by Monte Carlo simulations the performance of the proposed subspace timing and channel estimation scheme under different channel conditions. The signature sequences are binary and are randomly generated. The channel coefficients $\alpha_{k,m}$ are generated according to the complex Gaussian distribution with zero mean and unit variance, i.e., Rayleigh fading is assumed. For the chip waveform, we employ a raised-cosine waveform with roll-off factor 0.9. We use samples from 200 symbols to estimate the correlation matrix. For simplicity, we assume that the number of users, K , is known and that each user contributes at most three dominant vectors ($L = 1$). The dimension P of the signal subspace is taken to be $(2L + 1)K$. Up to 1500 realizations, each containing 500 BPSK data symbols, are used to obtain all the results. To look at the performance of the subspace method under various channel conditions, we consider the six sample systems listed in Table I.

The ‘‘near-far ratio’’ (NFR) is the ratio of the average received power of each interferer to that of the desired user [8].



(a)



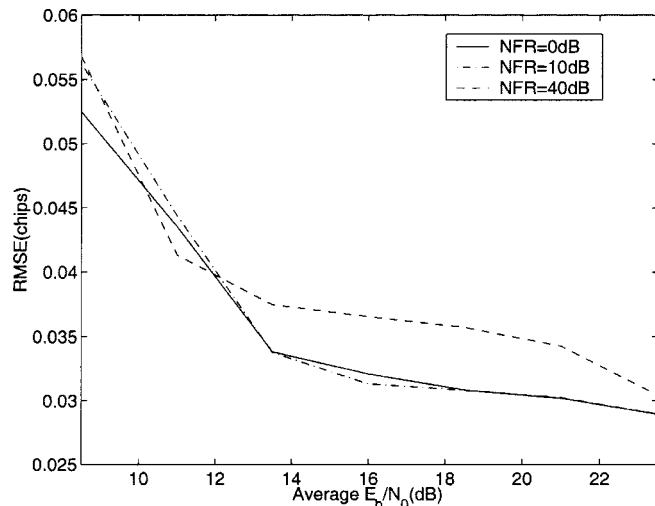
(b)

Fig. 2. Probability of acquisition. (a) Systems A, C, E. (b) Systems B, D, F.

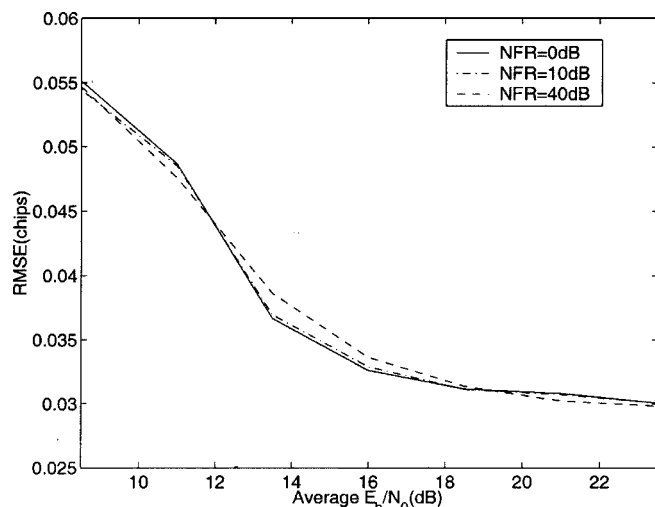
A. Timing and Channel Estimation

First, we employ the joint timing and channel estimation scheme in Section IV for the six sample systems. When the timing estimate obtained is more than $0.5T_c$ away from the true value, we assume that an acquisition failure occurs and that estimate is called an *outlier* [7]. Fig. 2 summarizes the probability of acquisition when the average signal-to-noise ratio (\bar{E}_b/N_0) of the desired user increases for the six sample systems. We observe that the probability of acquisition can be made close to 1 (within 0.25%) when \bar{E}_b/N_0 is larger than 15 dB for all six systems. We exclude the outliers from all the results presented below. The root-mean-squared (RMS) errors of the timing estimation for the six systems are plotted in Fig. 3. We can see from the figure that the timing estimation is near-far resistant to a certain extent. For $M = 2$ and $N = 16$, the RMS errors for different NFRs are similar. However, the effect of the finite-length truncation of the chip waveform starts to appear for the severe near-far situation in System E, and this causes the RMS error to increase.

After acquiring the timing, we adjust the sampling time according to the estimated value of T_1 to resample the chip-



(a)



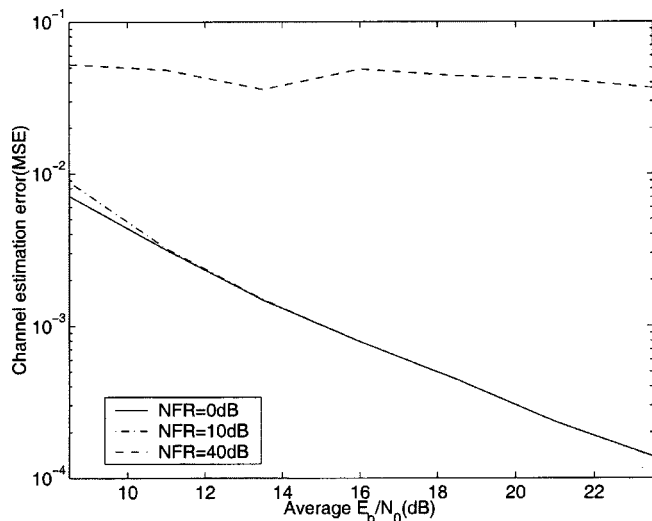
(b)

Fig. 3. Root-mean squared estimation error of T_1 . (a) Systems A, C, E. (b) Systems B, D, F.

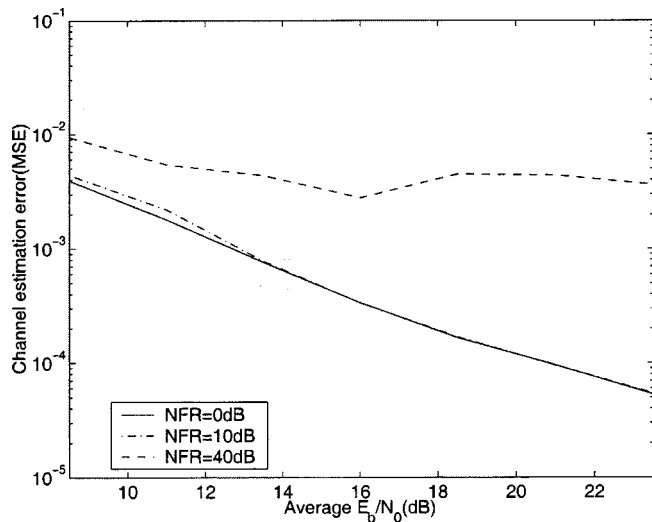
matched filter outputs and then perform the channel vector estimation described in Section IV. The reason for doing so is twofold: the intersymbol interference from the desired user is eliminated and the most of the signal energy can be collected so that the performance of the system can be improved. Fig. 4 shows the average normalized channel estimation error. We see that the channel estimation is resistant to moderate near-far effects ($\text{NFR} \leq 10$ dB). Under severe near-far situations ($\text{NFR} = 40$ dB), the channel estimation scheme fails.

B. Bit-Error Rate (BER)

We employ the timing and channel estimates obtained previously to construct the MMSE receiver described in Section III and investigate its BER performance. First, we compare the BER performance of the MMSE receiver with that of the matched filter followed by the maximal ratio combiner (MRC) [1] for the case of a single-user system. Differential encoding and decoding of the information data is employed at the output of the MRC. The results are shown in Fig. 5. Under the single-user condition, the MRC is optimal. It can be shown



(a)



(b)

Fig. 4. Mean-squared estimation error of d_1 . (a) Systems A, C, E. (b) Systems B, D, F.

easily that the weight vector for the MMSE receiver reduces to the MRC if perfect estimates of the correlation matrix and fading coefficient vector can be obtained. From Fig. 5, we see that the performance of the subspace method using the imperfect channel estimates is close to the optimal performance by the MRC with the exact channel information. The difference is less than 1 dB. An increase in the number of carriers M provides a larger degree of frequency diversity. Therefore, the system with $M = 4$ outperforms the system with $M = 2$.

Next, we consider the BER performance of the six sample systems. The results are shown in Figs. 6 and 7. We note that in all the cases, the MMSE receiver outperforms the MRC that assumes perfect knowledge of timing and channel information. This is because of the inability of the MRC to reject multiple-access interference (MAI). For moderate near-far situations ($NFR \leq 10$ dB) and a moderate range of \bar{E}_b/N_0 , the performance of the MMSE receiver is only 2–4 dB poorer than the single-user performance of the MRC with perfect channel knowledge. For severe near-far situations ($NFR = 40$ dB),

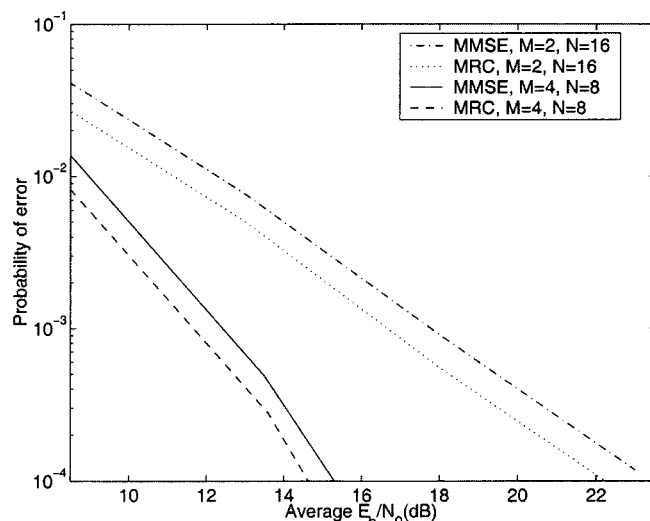
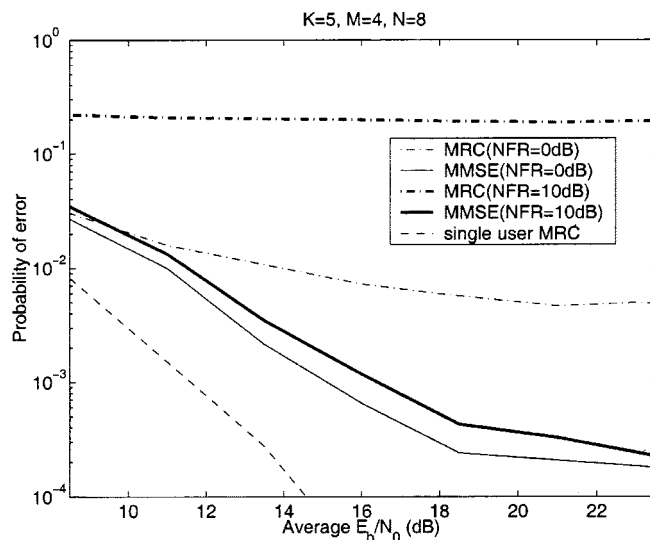
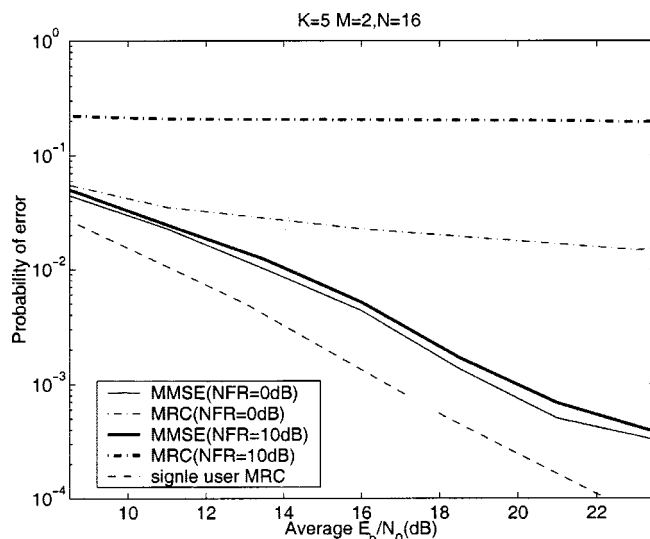


Fig. 5. BER performance for the single-user system.



(a)



(b)

Fig. 6. BER performance for Systems A, B, C, and D. (a) Systems A, C. (b) Systems B, D.

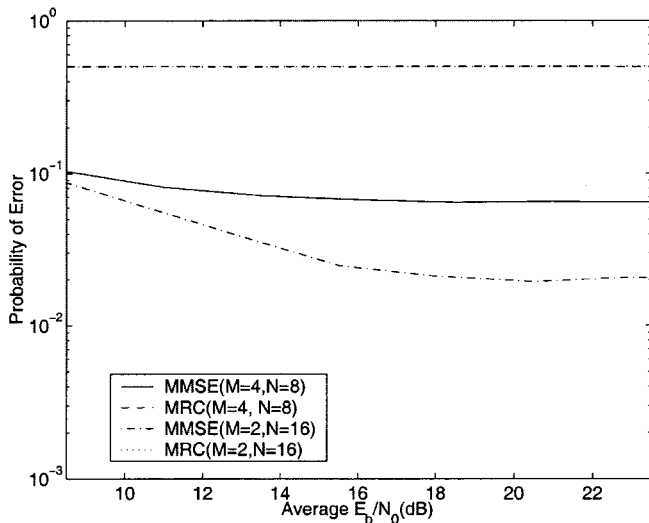


Fig. 7. BER performance for Systems E and F.

the poor channel estimates cause the MMSE receiver to fail. Error floors are observed in all cases indicating that the MMSE receiver is not near-far resistant [3]. This is due to the band-limited nature of the chip waveform (see Section VI for more discussion). Increasing the processing gain N increases the tolerance of the system toward MAI, while increasing the number of carriers M provides more frequency diversity. For a fixed total system bandwidth, a trade off must be made between the values of N and M depending on the near-far ratio, the number of active users, and the SNR of the desired user.

VI. FINITE-LENGTH TRUNCATION OF CHIP WAVEFORM

In the development of the subspace-based MMSE receiver, we have assumed that each user contributes at most $2L + 1$ linearly independent vectors to the received vector \mathbf{r} . As stated before, this is only an approximation (unless all users are chip-synchronous) to the MC-DS-CDMA system because the chip waveform is not time-limited. In this section, we consider the fact that each user is actually contributing an infinite number of vectors to \mathbf{r} and investigate the resulting effect on the performance of the proposed subspace MMSE receiver. We note that the discussions below also apply, with only slight modifications, to many subspace-based estimation and detection scheme for DS-CDMA systems with band-limited chip waveforms.

First, since the signal vectors from all the users span the entire $2MN$ -dimensional space,⁷ the desired signal vector cannot be independent of the signal vectors from the other users. This implies that the near-far resistance of the MMSE receiver is zero [5], regardless of the finite-length truncation approximation we made in Sections III and IV. However, near-far resistance measures the system performance under the unlikely situation where the interferer powers are unbounded. In practice, the near-far problem is far more modest. It is shown by the numerical results in Section V that the subspace-based MMSE receiver gives

reasonably good performance. We can still obtain a large performance gain over the conventional matched filter receiver by employing the MMSE detection technique.

As mentioned in Section III, the finite-length truncation of the chip waveform is a reasonable approximation when the chip waveform decays fast enough. Here, we characterize this claim by using results from matrix perturbation theory [18]. To this end, we treat the vectors in (14) from symbols other than $\{b_i^{(k)}\}_{i=-L}^L$, for $k = 1, 2, \dots, K$, as *perturbations* to the *unperturbed* observation vector \mathbf{r} obtained by the finite-length truncation approximation in (15). The correlation matrix \mathbf{R} of the unperturbed vector \mathbf{r} is called the *unperturbed correlation matrix*. We observe samples of the perturbed vector and form an estimation of the *perturbed correlation matrix* $\hat{\mathbf{R}}$ from the samples. For simplicity, we assume that a perfect estimate of the perturbed correlation matrix is obtained from the samples. The effect of finite samples on the performance of channel estimation can be found in [9] and [10].

If the number of users in the system is known and no user is chip-synchronous to the start of the observation interval, then $P = (2L + 1)K$, and its value can be chosen by setting L . We decompose the $2MN$ -dimensional space into a P -dimensional *unperturbed signal subspace* and a $(2MN - P)$ -dimensional *unperturbed noise subspace* as in Section III. We perform a similar decomposition based on the perturbed correlation matrix. For example, a *perturbed signal subspace* is obtained by taking the span of the eigenvectors corresponding to the P largest eigenvalues of the perturbed correlation matrix. The perturbation vectors change the eigenstructure of the unperturbed correlation matrix, which is the basis of the subspace technique. Since we perform EVD based on the perturbed correlation matrix, the performance of the subspace technique will strongly depend on the perturbations. As long as the unperturbed subspaces are not seriously altered, it is possible to achieve reliable estimation and detection. This is the case when a fast decaying chip waveform is employed and the near-far problem is not too severe. On the other hand, if the perturbations are strong enough to severely alter the eigenstructure to an extent that the desired signal vector \mathbf{p}_1 is better approximated by the perturbed noise subspace than by the perturbed signal subspace, the subspace technique will break down. This phenomenon is known as *subspace swap* [15], [16]. The goal of the following analysis is to characterize the effect of perturbations on the estimations of the signal and noise subspaces.

A. Inseparable Signal and Noise Subspaces

First, we look at the effect of the perturbations on the subspace decomposition in Section III. Let \mathbf{u}_i , for $i = 1, 2, \dots, 2MN$, denote the eigenvectors corresponding to the eigenvalues (in descending order) of the unperturbed correlation matrix \mathbf{R} . The first P eigenvectors span the unperturbed signal subspace, and the remaining eigenvectors span the unperturbed noise subspace. We can rewrite (18) as

$$\mathbf{R} = \sum_{l=1}^P \lambda_l \mathbf{u}_l \mathbf{u}_l^H + \sum_{l=P+1}^{2MN} \sigma^2 \mathbf{u}_l \mathbf{u}_l^H. \quad (30)$$

⁷The span of the signal vectors depends on the chip waveform and the delays of the users. With a band-limited chip waveform and random delays, it is likely that the span will be the entire space.

Now, we note that the perturbation vectors in (14), denoted by \mathbf{p}_k , for $k \geq P + 1$, can be written as

$$\mathbf{p}_k = b_k \sum_{l=1}^{2MN} c_{k,l} \mathbf{u}_l. \quad (31)$$

By defining a $2MN$ -by- $2MN$ matrix $\mathbf{\Xi}$, whose (i, j) th element, for $i, j = 1, 2, \dots, 2MN$, is given by $\varepsilon_{i,j} = \sum_{k=P+1}^{\infty} c_{k,i} c_{k,j}^*$, and using (31), we obtain the perturbed correlation matrix $\tilde{\mathbf{R}}$ as

$$\tilde{\mathbf{R}} = \mathbf{R} + \mathbf{E} \quad (32)$$

where

$$\mathbf{E} = \sum_{i=1}^{2MN} \sum_{j=1}^{2MN} \varepsilon_{i,j} \mathbf{u}_i \mathbf{u}_j^H = [\mathbf{U}_s \quad \mathbf{U}_n] \mathbf{\Xi} [\mathbf{U}_s \quad \mathbf{U}_n]^H. \quad (33)$$

We can regroup the terms of $\tilde{\mathbf{R}}$ as

$$\tilde{\mathbf{R}} = \mathbf{R}_s + \mathbf{R}_n + \mathbf{R}_o \quad (34)$$

where

$$\mathbf{R}_s = \sum_{l=1}^P \lambda_l \mathbf{u}_l \mathbf{u}_l^H + \sum_{i=1}^P \sum_{j=1}^P \varepsilon_{i,j} \mathbf{u}_i \mathbf{u}_j^H \quad (35)$$

$$\mathbf{R}_n = \sum_{l=P+1}^{2MN} \sigma^2 \mathbf{u}_l \mathbf{u}_l^H + \sum_{i=P+1}^{2MN} \sum_{j=P+1}^{2MN} \varepsilon_{i,j} \mathbf{u}_i \mathbf{u}_j^H \quad \text{and} \quad (36)$$

$$\mathbf{R}_o = \sum_{i=1}^P \sum_{j=P+1}^{2MN} \varepsilon_{i,j} \mathbf{u}_i \mathbf{u}_j^H + \sum_{i=P+1}^{2MN} \sum_{j=1}^P \varepsilon_{i,j} \mathbf{u}_i \mathbf{u}_j^H. \quad (37)$$

We denote the column space of a matrix \mathbf{A} by $\mathcal{R}(\mathbf{A})$. From (30), we see that $\mathcal{R}(\mathbf{U}_s)$ and $\mathcal{R}(\mathbf{U}_n)$ are invariant subspaces⁸ of \mathbf{R} since $\mathbf{U}_s^H \mathbf{R} \mathbf{U}_n = \mathbf{0}$. Also, they are invariant by \mathbf{R}_s and \mathbf{R}_n because of (35) and (36). However, one can easily see from (37) that $\mathcal{R}(\mathbf{U}_s)$ and $\mathcal{R}(\mathbf{U}_n)$ are not invariant by \mathbf{R}_o . Thus, they are not invariant subspaces of $\tilde{\mathbf{R}}$. Since any subspace spanned by a subset of the eigenvectors of $\tilde{\mathbf{R}}$ is an invariant subspace of $\tilde{\mathbf{R}}$, neither $\mathcal{R}(\mathbf{U}_s)$ nor $\mathcal{R}(\mathbf{U}_n)$ is spanned by some subset of the eigenvectors of $\tilde{\mathbf{R}}$. Hence, it is impossible to obtain the *unperturbed* signal and noise subspaces from an EVD of $\tilde{\mathbf{R}}$, which is what we observe. Each of the estimated signal and noise subspaces will always have nonzero projections onto both the unperturbed signal and noise subspaces.

B. Subspace Perturbation

Although the unperturbed signal and noise subspaces cannot be separated from an EVD of $\tilde{\mathbf{R}}$, the perturbed signal and noise subspaces can still be good approximations of their unperturbed counterparts (provided that the perturbations are small) since subspaces spanned by eigenvectors are relatively insensitive to

⁸A subspace \mathcal{X} is an *invariant subspace* of a matrix \mathbf{A} if $\mathbf{A}\mathcal{X} \subset \mathcal{X}$. The following result from [18, p. 220] can be employed to characterize an invariant subspace. Let the columns of \mathbf{X} be linearly independent and let the columns of \mathbf{Y} span $\mathcal{R}(\mathbf{X})^\perp$. Then, $\mathcal{R}(\mathbf{X})$ is an invariant subspace of \mathbf{A} if and only if $\mathbf{Y}^H \mathbf{A} \mathbf{X} = \mathbf{0}$. In this case, $\mathcal{R}(\mathbf{Y})$ is an invariant subspace of \mathbf{A}^H .

perturbations in the correlation matrix [19], [20]. Intuitively, a fast decaying chip waveform in a not too severe near-far situation gives rise to small perturbations in the correlation matrix. Hence, under this condition, the subspace MMSE receiver should give a good performance. The simulation results in Section V confirm this observation.

To develop measures to appraise the reliability of the channel estimation in Section IV using the perturbed subspaces, we need to first establish a measure of “difference” between two subspaces. First, let us decompose $\tilde{\mathbf{R}}$ as in (18) and obtain a similar EVD of $\tilde{\mathbf{R}}$ as below

$$\tilde{\mathbf{R}} = [\tilde{\mathbf{U}}_s \quad \tilde{\mathbf{U}}_n] \begin{bmatrix} \tilde{\mathbf{\Lambda}}_s & \\ & \tilde{\mathbf{\Lambda}}_n \end{bmatrix} \begin{bmatrix} \tilde{\mathbf{U}}_s^H \\ \tilde{\mathbf{U}}_n^H \end{bmatrix}. \quad (38)$$

In the following discussion, we focus on the noise subspaces. An argument for the signal subspaces can be obtained likewise.⁹ A commonly used measure of difference between two subspaces is given by the *canonical angles* between the two subspaces [18], [19], [21] (see the Appendix for the definition and properties of canonical angles). The smaller the angles, the closer are the two subspaces. Here, we employ the canonical angles to mathematically describe the perturbation effect on the noise subspace. It can be shown [18, p. 43] that the sines of the canonical angles between the unperturbed noise subspace $\mathcal{R}(\mathbf{U}_n)$ and the perturbed noise subspace $\mathcal{R}(\tilde{\mathbf{U}}_n)$ are the nonzero *singular values* of the matrix $\mathbf{U}_n^H \tilde{\mathbf{U}}_s$. Hence, if we take the canonical angles to form a diagonal matrix $\Theta(\mathcal{R}(\mathbf{U}_n), \mathcal{R}(\tilde{\mathbf{U}}_n))$, then

$$\|\sin \Theta(\mathcal{R}(\mathbf{U}_n), \mathcal{R}(\tilde{\mathbf{U}}_n))\| = \|\mathbf{U}_n^H \tilde{\mathbf{U}}_s\| \quad (39)$$

where $\|\cdot\|$ denotes the 2-norm of a matrix. We note that the 2-norm of $\sin \Theta$ in (39) equals the sine of the largest canonical angle. We proceed to upper-bound this quantity. To do so, we first note that

$$\begin{aligned} \mathbf{U}_n^H \tilde{\mathbf{U}}_s \tilde{\mathbf{U}}_s^H &= \mathbf{U}_n^H \left(\tilde{\mathbf{U}}_s \tilde{\mathbf{\Lambda}}_s \tilde{\mathbf{U}}_s^H \right) \left(\tilde{\mathbf{U}}_s \tilde{\mathbf{\Lambda}}_s^{-1} \tilde{\mathbf{U}}_s^H \right) \\ &= \mathbf{U}_n^H \left(\tilde{\mathbf{R}} - \tilde{\mathbf{U}}_n \tilde{\mathbf{\Lambda}}_n \tilde{\mathbf{U}}_n^H \right) \left(\tilde{\mathbf{U}}_s \tilde{\mathbf{\Lambda}}_s^{-1} \tilde{\mathbf{U}}_s^H \right) \\ &= \left(\mathbf{U}_n^H \tilde{\mathbf{R}} \right) \left(\tilde{\mathbf{U}}_s \tilde{\mathbf{\Lambda}}_s^{-1} \tilde{\mathbf{U}}_s^H \right) \\ &= \left(\sigma^2 \mathbf{U}_n^H + \mathbf{\Gamma} [\mathbf{U}_s \quad \mathbf{U}_n]^H \right) \left(\tilde{\mathbf{U}}_s \tilde{\mathbf{\Lambda}}_s^{-1} \tilde{\mathbf{U}}_s^H \right) \end{aligned} \quad (40)$$

where $\mathbf{\Gamma}$ is the $(2MN - P)$ -by- $2MN$ submatrix of $\mathbf{\Xi}$ defined by $\mathbf{\Gamma} = [\mathbf{0}_{(2MN-P) \times P} \quad \mathbf{I}_{2MN-P}] \mathbf{\Xi}$.

The last equality in (40) is obtained by applying the orthogonal relations between the eigenvectors $\mathbf{u}_1, \mathbf{u}_2, \dots, \mathbf{u}_{2MN}$ to the decomposition of $\tilde{\mathbf{R}}$ in (34). From (39) and (40), we get

$$\begin{aligned} \|\sin \Theta(\mathcal{R}(\mathbf{U}_n), \mathcal{R}(\tilde{\mathbf{U}}_n))\| &= \|\mathbf{U}_n^H \tilde{\mathbf{U}}_s \tilde{\mathbf{U}}_s^H\| \\ &\leq \|\sigma^2 \mathbf{U}_n^H + \mathbf{\Gamma} [\mathbf{U}_s \quad \mathbf{U}_n]^H\| \|\tilde{\mathbf{U}}_s \tilde{\mathbf{\Lambda}}_s^{-1} \tilde{\mathbf{U}}_s^H\| \\ &\leq \frac{\sigma^2 + \|\mathbf{\Gamma}\|}{\tilde{\lambda}_P} \leq \frac{\sigma^2 + \|\mathbf{\Xi}\|}{\tilde{\lambda}_P} \end{aligned} \quad (41)$$

⁹It turns out that $\|\sin \Theta(\mathcal{R}(\mathbf{U}_s), \mathcal{R}(\tilde{\mathbf{U}}_s))\| = \|\mathbf{U}_n^H \tilde{\mathbf{U}}_s\| \leq (\sigma^2 + \mu_1) / (\lambda_P + \mu_{2MN})$ as in (39) and (43).

where $\tilde{\lambda}_P$ is the P th eigenvalue of $\tilde{\mathbf{R}}$. Furthermore, since \mathbf{E} is semi-positive definite, it can be shown [18] that

$$\lambda_P + \mu_{2MN} \leq \tilde{\lambda}_P \leq \lambda_P + \mu_1 \quad (42)$$

where $\mu_1 = \|\mathbf{\Xi}\|$ and $\mu_{2MN} \geq 0$ are the largest and smallest eigenvalues of $\mathbf{\Xi}$, respectively. Hence, it follows that

$$\|\sin \Theta(\mathcal{R}(\mathbf{U}_n), \mathcal{R}(\tilde{\mathbf{U}}_n))\| \leq \frac{\sigma^2 + \mu_1}{\lambda_P + \mu_{2MN}}. \quad (43)$$

From (43), the canonical angles between the unperturbed and perturbed noise subspaces are small when the chip waveform decays fast and the power of the interferers are not too large. In particular, when $s_n = \|\sin \Theta(\mathcal{R}(\mathbf{U}_n), \mathcal{R}(\tilde{\mathbf{U}}_n))\| < 1$, the two noise subspaces are *acute* [18]. If the two subspaces are acute, there is no vector in $\mathcal{R}(\mathbf{U}_n)$ that is orthogonal to $\mathcal{R}(\tilde{\mathbf{U}}_n)$ and vice versa. A sufficient condition for acute perturbation can be $\mu_1 - \mu_{2MN} < \lambda_P - \sigma^2$, or simply $\|\mathbf{\Xi}\| < \lambda_P - \sigma^2$. Hence, we want $\|\mathbf{\Xi}\|$ (or $\|\mathbf{E}\|$) small so that the perturbed noise subspace is close to its unperturbed counterpart.

It can be shown [18, p. 255] that when the perturbed and unperturbed subspaces are acute, there is a matrix \mathbf{P} such that $\mathcal{R}(\tilde{\mathbf{U}}_n) = \mathcal{R}(\mathbf{U}_n + \mathbf{U}_s \mathbf{P})$. Moreover, $\|\mathbf{P}\| = \sqrt{s_n^2 / (1 - s_n^2)}$. In other words, there exists a nonsingular matrix \mathbf{A} such that

$$\tilde{\mathbf{U}}_n \mathbf{A} = \mathbf{U}_n + \Delta \mathbf{U}_n \quad (44)$$

where $\|\Delta \mathbf{U}_n\|$ decreases as the canonical angles get smaller. Moreover

$$\tilde{\mathbf{\Lambda}}_n = \sigma^2 \mathbf{I} + \Delta \mathbf{\Lambda}_n \quad (45)$$

where $\|\Delta \mathbf{\Lambda}_n\| \leq \|\mathbf{\Xi}\|$ [18, p. 203]. We will use these two facts in the next section.

C. Channel Estimation Error Analysis

Using the subspace perturbation result in the previous section, we can develop a first-order analysis of the channel estimation error due to the finite-length truncation effect. We see from Section III that the MMSE receiver relies on the accuracy of the estimation of the desired user channel vector \mathbf{d}_1 . Hence, the error in $\tilde{\mathbf{d}}_1$ provides us a good indication of the effect of the finite-length truncation approximation on the subspace MMSE receiver. Based on (44) and (45), we derive the first-order error [17] on $\tilde{\mathbf{d}}_1$ assuming that the canonical angles between the unperturbed and perturbed noise subspaces are small.

Instead of (24), we actually solve the following systems of equations to obtain the desired user channel vector estimate $\tilde{\mathbf{d}}_1$:

$$\tilde{\mathbf{U}}_n^H \mathbf{V}_1 \tilde{\mathbf{d}}_1 = \mathbf{0}. \quad (46)$$

Unfortunately, a nontrivial solution to this equation may not exist. So, we use the least square approach as in Section IV. We assume that the value of $\|\tilde{\mathbf{U}}_n^H \mathbf{V}_1 \tilde{\mathbf{d}}_1\|$ obtained by the least square solution is close to zero. Since both \mathbf{d}_1 and $\tilde{\mathbf{d}}_1$ can only be determined up to a multiplicative constant, we normalize their norms to one and define the error in the estimate to be

$$\Delta \mathbf{d}_1 = e^{j\phi} \tilde{\mathbf{d}}_1 - \mathbf{d}_1 \quad (47)$$

where ϕ minimizes $\|e^{j\phi} \tilde{\mathbf{d}}_1 - \mathbf{d}_1\|$. Substituting this $\tilde{\mathbf{d}}_1$ into (46), we have

$$(\mathbf{A}^H)^{-1} e^{-j\phi} (\mathbf{U}_n + \Delta \mathbf{U}_n)^H \mathbf{V}_1 (\mathbf{d}_1 + \Delta \mathbf{d}_1) \approx \mathbf{0}. \quad (48)$$

Since \mathbf{A} is nonsingular, (48) implies that

$$\mathbf{U}_n^H \mathbf{V}_1 \Delta \mathbf{d}_1 + \Delta \mathbf{U}_n^H \mathbf{V}_1 \mathbf{d}_1 + \Delta \mathbf{U}_n^H \mathbf{V}_1 \Delta \mathbf{d}_1 \approx \mathbf{0}. \quad (49)$$

Neglecting the second-order term $\Delta \mathbf{U}_n^H \mathbf{V}_1 \Delta \mathbf{d}_1$, we get, based on the least square nature of the solution

$$\Delta \mathbf{d}_1 \approx -(\mathbf{U}_n^H \mathbf{V}_1)^\dagger \Delta \mathbf{U}_n^H \mathbf{V}_1 \mathbf{d}_1 \quad (50)$$

where \dagger denotes the Moore–Penrose pseudo-inverse of a matrix.

What remains is obtaining a first-order approximate expression of $\Delta \mathbf{U}_n^H$, which can be obtained by premultiplying (38) by $\tilde{\mathbf{U}}_n^H$

$$\begin{aligned} \tilde{\mathbf{U}}_n^H \tilde{\mathbf{R}} &= \tilde{\mathbf{\Lambda}}_n \tilde{\mathbf{U}}_n^H \\ (\mathbf{A}^H)^{-1} (\mathbf{U}_n + \Delta \mathbf{U}_n)^H (\mathbf{R} + \mathbf{E}) & \\ &= (\sigma^2 \mathbf{I} + \Delta \mathbf{\Lambda}_n) (\mathbf{A}^H)^{-1} (\mathbf{U}_n + \Delta \mathbf{U}_n)^H \\ \mathbf{U}_n^H \mathbf{R} + \mathbf{U}_n^H \mathbf{E} + \Delta \mathbf{U}_n^H \mathbf{R} + \Delta \mathbf{U}_n^H \mathbf{E} & \\ &= \sigma^2 \mathbf{U}_n^H + \mathbf{A}^H \Delta \mathbf{\Lambda}_n (\mathbf{A}^H)^{-1} \mathbf{U}_n^H + \sigma^2 \Delta \mathbf{U}_n^H \\ &\quad + \mathbf{A}^H \Delta \mathbf{\Lambda}_n (\mathbf{A}^H)^{-1} \Delta \mathbf{U}_n^H \\ \mathbf{\Gamma} [\mathbf{U}_s \quad \mathbf{U}_n]^H + \Delta \mathbf{U}_n^H \mathbf{R} + \Delta \mathbf{U}_n^H \mathbf{E} & \\ &= \mathbf{A}^H \Delta \mathbf{\Lambda}_n (\mathbf{A}^H)^{-1} \mathbf{U}_n^H + \sigma^2 \Delta \mathbf{U}_n^H \\ &\quad + \mathbf{A}^H \Delta \mathbf{\Lambda}_n (\mathbf{A}^H)^{-1} \Delta \mathbf{U}_n^H \quad \text{and} \\ \Delta \mathbf{U}_n^H (\mathbf{R} - \sigma^2 \mathbf{I}) &\approx \mathbf{A}^H \Delta \mathbf{\Lambda}_n (\mathbf{A}^H)^{-1} \mathbf{U}_n^H - \mathbf{\Gamma} [\mathbf{U}_s \quad \mathbf{U}_n]^H \end{aligned} \quad (51)$$

where the second-order terms $\Delta \mathbf{U}_n^H \mathbf{E}$ and $\mathbf{A}^H \Delta \mathbf{\Lambda}_n (\mathbf{A}^H)^{-1} \Delta \mathbf{U}_n^H$ have been neglected. Post-multiplying both sides of (51) by $\mathbf{U}_s (\mathbf{\Lambda}_s - \sigma^2 \mathbf{I})^{-1} \mathbf{U}_s^H \mathbf{V}_1 \mathbf{d}_1$ and noting that $\mathbf{V}_1 \mathbf{d}_1$ lies in $\mathcal{R}(\mathbf{U}_s)$, we have

$$\Delta \mathbf{U}_n^H \mathbf{V}_1 \mathbf{d}_1 \approx -\mathbf{\Upsilon} (\mathbf{\Lambda}_s - \sigma^2 \mathbf{I})^{-1} \mathbf{U}_s^H \mathbf{V}_1 \mathbf{d}_1 \quad (52)$$

where $\mathbf{\Upsilon}$ is the $(2MN - P)$ -by- P submatrix of $\mathbf{\Gamma}$ defined by $\mathbf{\Upsilon} = \mathbf{\Gamma} [\mathbf{I}_P \quad \mathbf{0}_{P \times (2MN - P)}]^H$.

Finally, by substituting (52) back into (50), we get

$$\Delta \mathbf{d}_1 \approx (\mathbf{U}_n^H \mathbf{V}_1)^\dagger \mathbf{\Upsilon} (\mathbf{\Lambda}_s - \sigma^2 \mathbf{I})^{-1} \mathbf{U}_s^H \mathbf{p}_1. \quad (53)$$

From (53), we can see that the error in estimating \mathbf{d}_1 is determined by $\|\mathbf{\Xi}\|$ (more precisely $\|\mathbf{\Upsilon}\|$) and the projections of the desired signal vector onto the eigenvectors of the unperturbed signal subspace, scaled by the reciprocals of their corresponding eigenvalues. In practice, we can make $\|\mathbf{\Xi}\|$ small (relative to $\|\mathbf{R}\|$) by using a fast decaying chip waveform. Hence, the channel estimation error can be made small in moderate near–far situations. When the powers of the interferers increase, $\|\mathbf{\Xi}\|$ and the eigenvalues of the unperturbed subspaces increase at roughly the same rate. Hence, their effects on the estimation cancel one another [see (53)]. However, the increase in the interferer powers changes the structure of the signal subspace. In particular, \mathbf{p}_1 will now be more aligned with the eigenvector corresponding to a small eigenvalue. As a result, the estimation error increases as the near–far effect gets more severe.

To illustrate the discussion above with numerical examples, we reconsider Systems C and E in Section V. Here, we assume

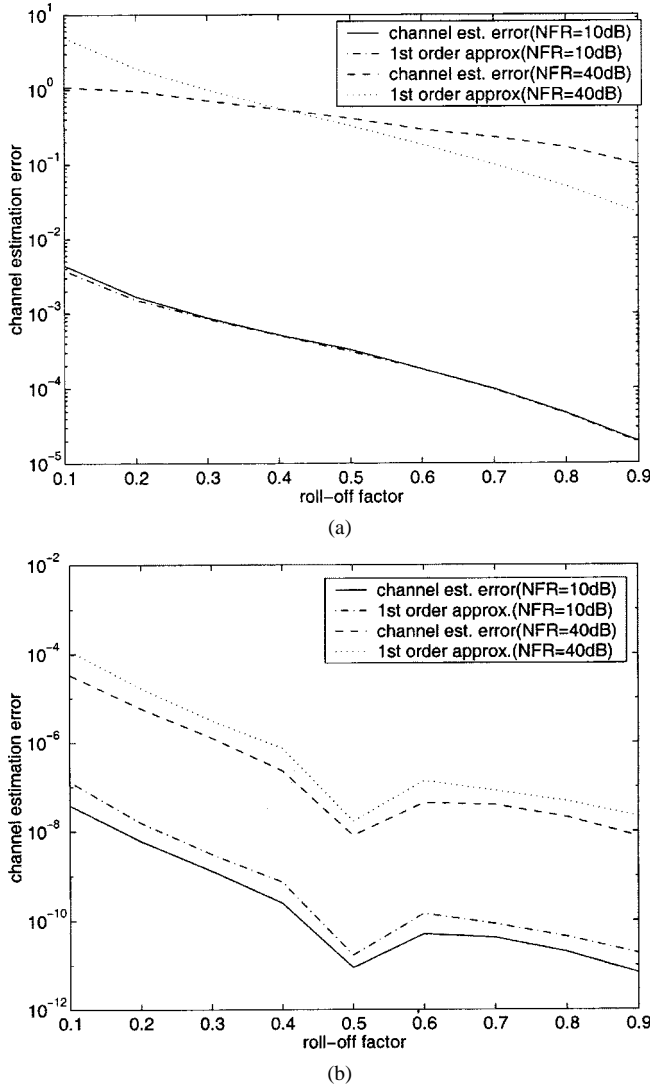


Fig. 8. Channel estimation error for Systems C and E. (a) $L = 1$. (b) $L = 3$.

that a perfect estimate of $\tilde{\mathbf{R}}$ is available and the receiver is synchronized to the desired user ($T_1 = 0$). We calculate the true value of $\|\Delta \mathbf{d}_1\|$ as defined in (47) and its first-order approximation given by (53) for raised-cosine chip waveforms with a roll-off factor ranging from 0.1 to 0.9 (fast decay). The results are shown in Fig. 8. First, we observe that the finite truncation effect is negligible ($\|\Delta \mathbf{d}_1\|$ is small) in the moderate near-far situation (NFR = 10 dB, $L = 1$). However, the effect becomes significant ($\|\Delta \mathbf{d}_1\|$ is large) in the severe near-far situation (NFR = 40 dB, $L = 1$). Also, note that “severity” of a near-far problem depends on L . It is observed that we can reduce the error due to the finite truncation effect by increasing L as long as the condition in (26) is maintained. Second, as the roll-off factor increases, the chip waveform decays faster and, hence, $\|\Delta \mathbf{d}_1\|$ decreases. Finally, we see from the results that the first-order approximation is very accurate for the moderate near-far case.

VII. CONCLUSIONS

In this paper, we have proposed a subspace-based MMSE multiuser detector for the multicarrier DS-CDMA system. To

implement the linear MMSE detector, the channel and timing information of the desired user is needed. We have presented a subspace-based blind algorithm for channel and timing estimation based on the finite-length truncation approximation of a chip waveform. The signal subspace estimated from the observed signal is different from that spanned by the signal vectors considered by the finite-length approximation. Therefore, the subspace-based technique inevitably suffers from a performance degradation. However, we have shown in numerical results that the proposed channel estimation scheme is robust to moderate near-far problems. Moreover, we have investigated the effect of band-limited chip waveforms on the proposed subspace-based channel estimation scheme based on the matrix perturbation approach. With slight modifications, our analysis can be directly applied to many subspace-based estimation and detection schemes, whether single-carrier or multicarrier.

APPENDIX

We briefly review some matrix perturbation theory results from [18] and [20] that we use in Section VI. First, we define the canonical angles between subspaces of the same dimension based on the following result.

Theorem 1 [20, p. 734]: Let $\mathcal{X}, \mathcal{Y} \in \mathbb{C}^n$ be subspace with $\dim(\mathcal{X}) = \dim(\mathcal{Y}) = l$. Let $2l \leq n$. Then there are unitary matrices $\mathbf{X} = [\mathbf{X}_1 \mathbf{X}_2]$ and $\mathbf{Y} = [\mathbf{Y}_1 \mathbf{Y}_2]$ such that $\mathcal{R}(\mathbf{X}_1) = \mathcal{X}$, $\mathcal{R}(\mathbf{Y}_1) = \mathcal{Y}$, and

$$\mathbf{Y}^H \mathbf{X} = \begin{bmatrix} \Phi & \Sigma & \mathbf{0} \\ -\Sigma & \Phi & \mathbf{0} \\ \mathbf{0} & \mathbf{0} & \mathbf{I}_{n-2l} \end{bmatrix} \quad (54)$$

where $\Phi = \text{diag}(\phi_1, \phi_2, \dots, \phi_l)$ and $\Sigma = \text{diag}(\sigma_1, \sigma_2, \dots, \sigma_l)$ have nonnegative diagonal elements. We note that $\Phi^H \Phi + \Sigma^H \Sigma = \mathbf{I}_l$, and $\phi_i^2 + \sigma_i^2 = 1$. This suggests the following definition of canonical angles.

Definition [18, p. 43]: The canonical angles between \mathcal{X} and \mathcal{Y} are the diagonal elements of the matrix $\Theta(\mathcal{X}, \mathcal{Y}) \triangleq \sin^{-1} \Sigma$.

What we are interested in under many circumstances is the sine of the largest canonical angle. It can be obtained as [18, p. 93] $\|\sin \Theta(\mathcal{X}, \mathcal{Y})\| = \|\Pi_{\mathcal{X}} - \Pi_{\mathcal{Y}}\|$, where $\Pi_{\mathcal{X}}$ and $\Pi_{\mathcal{Y}}$ are projections onto \mathcal{X} and \mathcal{Y} , respectively. The following relation is useful in calculating this value [18, p. 43]:

$$\|\Pi_{\mathcal{X}} - \Pi_{\mathcal{Y}}\| = \|\Pi_{\mathcal{X}^\perp} \Pi_{\mathcal{Y}}\| = \|\Pi_{\mathcal{Y}^\perp} \Pi_{\mathcal{X}}\| \quad (55)$$

where \perp denotes the orthogonal complement of a given subspace.

Now, we state an important characterization of “closeness” between two subspaces of the same dimension. Given a matrix \mathbf{A} , we denote its perturbation by $\tilde{\mathbf{A}} = \mathbf{A} + \mathbf{E}$. Also, let us denote the projection onto $\mathcal{R}(\mathbf{A})$ as Π and the projection onto $\mathcal{R}(\tilde{\mathbf{A}})$ as $\tilde{\Pi}$.

Theorem 2 [18, p. 137]: The following three statements are equivalent.

- 1) $\|\tilde{\Pi} - \Pi\| < 1$.
- 2) There is no vector in $\mathcal{R}(\tilde{\mathbf{A}})$ that is orthogonal to $\mathcal{R}(\tilde{\mathbf{A}})$ and vice versa.
- 3) $\text{rank}(\mathbf{A}) = \text{rank}(\tilde{\mathbf{A}}) = \text{rank}(\Pi \tilde{\mathbf{A}})$.

The notion of *acute* subspaces is characterized by the second condition of Theorem 2 [18, p. 151]. This is used in Section VI to derive the channel estimation error.

REFERENCES

- [1] S. Kondo and L. B. Milstein, "Performance of multicarrier DS CDMA systems," *IEEE Trans. Commun.*, vol. 44, pp. 238–246, Feb. 1996.
- [2] T. M. Lok, T. F. Wong, and J. S. Lehnert, "Blind adaptive signal reception for MC-CDMA systems in Rayleigh fading channels," *IEEE Trans. Commun.*, vol. 47, pp. 464–471, Mar. 1999.
- [3] S. Verdú, "Multiuser detection," *Advances in Statistical Signal Processing*, vol. 2, pp. 369–409, 1993.
- [4] U. Madhow, "Blind adaptive interference suppression for direct-sequence CDMA," *Proc. IEEE*, vol. 86, pp. 2049–2069, Oct. 1998.
- [5] U. Madhow and M. L. Honig, "MMSE interference suppression for direct-sequence spread-spectrum CDMA," *IEEE Trans. Commun.*, vol. 42, pp. 3178–3188, Dec. 1994.
- [6] S. Bensley and B. Aazhang, "Subspace-based channel estimation for code division multiple access communication systems," *IEEE Trans. Commun.*, vol. 44, pp. 1009–1020, Aug. 1996.
- [7] E. G. Ström, S. Parkvall, S. L. Miller, and B. E. Ottersen, "Propagation delay estimation in asynchronous direct-sequence code-division multiple access systems," *IEEE Trans. Commun.*, vol. 44, pp. 84–92, Jan. 1996.
- [8] —, "DS-CDMA synchronization in time-varying fading channels," *IEEE J. Select. Areas Commun.*, vol. 14, pp. 1636–1642, Oct. 1996.
- [9] H. Liu and G. Xu, "A subspace method for signature waveform estimation in synchronous CDMA systems," *IEEE Trans. Commun.*, vol. 44, pp. 1346–1354, Oct. 1996.
- [10] M. Torlak and G. Xu, "Blind multiuser channel estimation in asynchronous CDMA systems," *IEEE Trans. Signal Processing*, vol. 45, pp. 137–147, Jan. 1997.
- [11] X. Wang and H. V. Poor, "Blind equalization and multiuser detection in dispersive CDMA channels," *IEEE Trans. Commun.*, vol. 46, pp. 91–103, Jan. 1998.
- [12] —, "Blind multiuser detection: A subspace approach," *IEEE Trans. Inform. Theory*, vol. 44, pp. 677–690, Mar. 1998.
- [13] U. Madhow, "MMSE interference suppression for acquisition and demodulation of direct-sequence CDMA systems," *IEEE Trans. Commun.*, vol. 46, pp. 1065–1075, Aug. 1998.
- [14] G. W. Stewart, "An updating algorithm for subspace tracking," *IEEE Trans. Signal Processing*, vol. 40, pp. 96–105, Oct. 1992.
- [15] D. W. Tufts, A. C. Kot, and R. J. Vaccaro, "The threshold effect in signal processing algorithm which use an estimated subspace," in *SVD and Signal Processing, II: Algorithms, Analysis and Applications*. New York: Elsevier, 1991.
- [16] J. K. Thomas, L. L. Scharf, and D. W. Tufts, "The probability of a subspace swap in the SVD," *IEEE Trans. Signal Processing*, vol. 43, pp. 730–736, Mar. 1995.
- [17] F. Li and R. J. Vaccaro, "Unified analysis for DOA estimation algorithms in array signal processing," *Signal Processing*, vol. 25, pp. 147–169, Nov. 1991.
- [18] G. W. Stewart and J.-G. Sun, *Matrix Perturbation Theory*. New York: Academic, 1990.
- [19] P.-Å. Wedin, "Perturbation bounds in connection to singular value decomposition," *BIT*, vol. 12, pp. 99–111, 1972.
- [20] G. W. Stewart, "Error and perturbation bounds for subspaces associated with certain eigenvalue problems," *SIAM Rev.*, vol. 15, pp. 727–764, Oct. 1973.

- [21] B. D. Rao, "Perturbation analysis of an SVD-based linear prediction method for estimating the frequencies of multiple sinusoids," *IEEE Trans. Acoust., Speech., Signal Processing*, vol. 36, pp. 1026–1035, July 1988.



June Namgoong received the B.S. degree in electronic engineering from Inha University, Republic of Korea, in 1995, and the M.S.E.E. degree in electrical and computer engineering from Purdue University, West Lafayette, IN, in 1999.

From 1995 to 1997, he served in the R.O.K. Army. Since 1998, he has been a Research Assistant in the School of Electrical and Computer Engineering at Purdue University. His current research interests include spread-spectrum communications.



Tan F. Wong (M'97) received the B.Sc. degree (first class honors) in electronic engineering from the Chinese University of Hong Kong, in 1991, and the M.S.E.E. and Ph.D. degrees in electrical engineering from Purdue University, West Lafayette, IN, in 1992 and 1997, respectively.

He was a Research Engineer working on the high-speed wireless networks project in the Department of Electronics at Macquarie University, Sydney, Australia. He also served as a Postdoctoral Research Associate in the School of Electrical and Computer Engineering at Purdue University. He is currently an Assistant Professor of Electrical and Computer Engineering at the University of Florida, Gainesville. His research interests include spread-spectrum communication systems, multiuser communications, and wireless cellular networks.



James S. Lehnert (S'83–M'84–SM'95–F'00) received the B.S. (highest honors), M.S., and Ph.D. degrees in electrical engineering from the University of Illinois at Urbana-Champaign in 1978, 1981, and 1984, respectively.

From 1978 to 1984, he was a Research Assistant at the Coordinated Science Laboratory, University of Illinois, Urbana. He was a University of Illinois Fellow from 1978 to 1979 and an IBM Predoctoral Fellow from 1982 to 1984. He has held summer positions at Motorola Communications, Schaumburg, IL, in the Data Systems Research Laboratory and Harris Corporation, Melbourne, FL, in the Advanced Technology Department. He is currently a Professor of Electrical and Computer Engineering at Purdue University, West Lafayette, IN.

Dr. Lehnert has served as Editor for Spread Spectrum for the IEEE TRANSACTIONS ON COMMUNICATIONS and as Guest Editor for the IEEE JOURNAL ON SELECTED AREAS IN COMMUNICATIONS.